The Dubins Traveling Salesman Problem with Neighborhoods in the Three-Dimensional Space

Petr Váňa, Jakub Sláma, Jan Faigl

***Abstract*— We introduce an extension of the Dubins Traveling Salesman Problem with Neighborhoods into the 3D space in which a fixed-wing aerial vehicle is requested to visit a set of target regions while the vehicle motion constraints are satisfied, i.e., the minimum turning radius and maximum climb and dive angles. The primary challenge is to address both the combinatorial optimization part of finding the sequence of target visits and the continuous optimization part of the final trajectory determination. Due to its high complexity, we propose to address both parts of the problem separately by a decoupled approach in which the sequence is determined by a new distance function designed explicitly for the utilized 3D Dubins Airplane model. The final trajectory is then found by a local optimization which improves the solution quality. The proposed approach provides significantly better solutions than using Euclidean distance in the sequencing part of the problem. Moreover, the found solutions are of the competitive quality to the sampling-based algorithm while its computational requirements are about two orders of magnitude lower.**

I. Introduction

In surveillance missions for a fixed-wing Unmanned Aerial Vehicle (UAV), the vehicle is requested to visit a given set of target locations to collect the required data. For the curvature-constrained Dubins vehicle in 2D, the trajectory planning problem can be formulated as the *Dubins Traveling Salesman Problem* (DTSP) [1] which stands to find a shortest closed-loop trajectory visiting all the given locations. A sub-problem of the DTSP is to determine heading angles at the target locations which is a continuous optimization problem called the Dubins Touring Problem in [2]. Moreover, relaxed target locations based on the sensor model are considered in the DTSP with Neighborhoods (DTSPN) [3] which is motivated by surveillance missions with a camera sensor [4] or by data gathering in wireless networks [5].

In this paper, we extend the DTSPN into the three-dimensional space that is called the **3D Dubins Traveling Salesman Problem with Neighborhoods** (3D-DTSPN). The targets are represented by 3D regions, e.g., cylindrical regions are shown in Fig. 1. Although the extension may seem straightforward, new challenges arise from the motion constraints that are the limited climb and dive angles. In particular, we utilize the *Dubins Airplane model* [6] for the trajectory generation between two configurations of the vehicle. Thus, the 3D-DTSPN stands to find configurations visiting the target regions such that the resulting trajectory connecting the configurations is the shortest possible.

The presented work has been supported by the Czech Science Foundation (GAČR) under research project No. 16-24206S.

The authors are with the Faculty of Electrical Engineering, Czech Technical University in Prague, Technická 2, 166 27 Prague, Czech Republic {vanapet1|slamajak|faiglj}@fel.cvut.cz

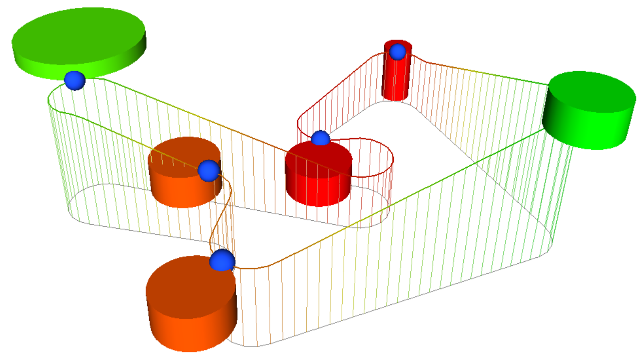

Fig. 1. An instance of the 3D Dubins Traveling Problem with Neighborhoods (3D-DTSPN). The cylinders stand for the target regions and the small blue spheres represent the determined locations of visits to the targets.

A simple approach to address the 3D-DTSPN is to extend the existing sampling-based methods for the DTSPN [4], [7]. However, both the waypoint positions and heading angles need to be sampled which makes the method quickly computationally intractable for larger instances, because the original problem is further transformed into a larger instance of the TSP.

Therefore, we propose to address the introduced 3D-DTSPN by a decoupled approach adopted from [1] in which the sequence of visits to the targets is determined by the Euclidean TSP. This approach is applicable even for the 3D-DTSPN; however, it does not consider the limited pitch angle, and thus in some cases, additional spiral segments need to be inserted to gain the required altitude, which prolongs the solution. To address this drawback of the decoupled approach, we propose a modified distance function that estimates the length of the 3D trajectory for the *Dubins Airplane model* more accurately. Finally, the trajectory connecting the target regions is optimized using the *Local Iterative Optimization* (LIO) algorithm [8] which can find a local optimum for the given sequence of visits to the target regions. Based on the numerical evaluation, the proposed approach finds solutions with competitive solution quality to the sampling-based approach, but with about two orders of magnitude lower computational requirements.

The remainder of the paper is organized as follows. Related work is summarized in the next section, and the 3D-DTSPN is formally introduced in Section III. A sampling-based approach together with the computing 3D trajectory based on the *Dubins Airplane model* is described in Section IV. The proposed decoupled approach is presented in Section V and it is compared with the sampling-based approach in Section VI. The final remarks are in Section VII.

II. RELATED WORK

Curvature-constrained path planning in 2D is studied since 1957 when L. E. Dubins addressed the shortest path planning problem between two points with prescribed heading angles. Such a path, further denoted as the Dubins maneuver, is one of CSC or CCC types, where S is a straight line segment and C is a circle segment with the minimum turning radius [9]. The CCC maneuver may exist only if the target locations are closer than four times the radius [10]; otherwise, the distance function is continuous and locally strictly convex [11].

The herein studied problem originates from the *Dubins Traveling Salesman Problem* (DTSP) [1] which stands to find a shortest curvature constrained path visiting the given set of target locations. Since a closed-form solution of the Dubins maneuver exists, the DTSP reduces to determine the sequence of visits and heading angles. If the target locations are allowed to be visited from their vicinity, the problem is called the Dubins TSP with Neighborhoods (DTSPN) [3]. Both of the variants are known to be NP-hard [12].

Various approaches for the DTSP(N) have been proposed that can be divided into four groups: decoupled, sampling-based, evolutionary, and unsupervised learning based approaches. In decoupled approaches, the sequence of the visits to the targets is determined based on the solution of the Euclidean TSP, and the heading angles are determined by various approaches, e.g., [1], [13], [14], [15] and the solution can be further improved by a post-processing procedure, e.g., by the *Local Iterative Optimization* (LIO) [8]. Sampling-based approaches [4], [16] tackle the DTSP(N) by sampling possible visiting configurations which enables to transform the problem into the Asymmetric TSP and solve it by existing algorithms, such as Concorde [17] or LKH solver [18]. Evolutionary algorithms use various mutation and crossover operators to improve the current population [19] and allow to utilize a local optimization procedure [20]. Finally, principles of unsupervised learning have been applied in [21], [22].

If the travel budget of the vehicle is limited, the problem can be formulated as the Dubins Orienteering Problem (DOP) without [23], [24] or with [25], [26] Neighborhoods. Extension of the DOP into 3D [27] is based on similar ideas as in this paper, i.e., the *Dubins Airplane model* [28].

In this paper, we extend the DTSP(N) into the three-dimensional space which requires a more complex model of the fixed-wing vehicle. A curvature-constrained trajectory in 3D is studied in [29], where the authors proved that the optimal solution could be CSC/CCC maneuver or helicoidal arc, where S is a straight line, and C is a circular arc segment. Such a strong theoretical result is in correspondence to the Dubins maneuver in 2D which is a special case of the 3D maneuver in the plane. However, two circle segments do not always lie in the same plane which makes the trajectory planning in 3D challenging. In [30], a path generation algorithm based on 2D Dubins maneuvers is proposed to satisfy the requested constraints. Further, a numerical method based on 3D geometry [31] is claimed to provide the optimal trajectory connecting two waypoints in about one second.

In the 3D, a fixed-wing vehicle is limited by the minimal and maximal pitch angle. Thus, the *Dubins Airplane model* is introduced [28] in which the vertical and horizontal constraints are defined independently, and the pitch angle can be changed abruptly. Although a sudden change of the pitch angle evidently violates motion constraints, the model seems to be a suitable approximation for fixed-wing vehicles with a small pitch angle range. A trajectory generation for this model is derived from the 2D Dubins maneuver generation. In [6], the *Dubins Airplane model* is adjusted for a small fixed-wing UAV. The trajectory generation procedure [6] is utilized in this paper.

In the Dubins-Helix model [32], spiral (helix) segments enable to have smaller radius projected to a horizontal plane than the actual minimum turning radius of the vehicle, and thus the model allows shorter trajectories than the *Dubins Airplane model*. However, it performs sharp turn maneuvers during altitude changes which push the vehicle to its limits. Alternatively, the problem can be addressed by utilizing parametric curves, e.g., quadratic Bézier curves [33], [34].

Although multiple approaches to 3D trajectory planning involving fixed-wing UAV exist, the TSP-based planning for the 3D *Dubins Airplane model* has not been addressed before. Therefore, we propose to leverage on the idea of the decoupled solution and utilize a decoupled approach for the 3D-DTSPN based on a novel distance function for finding a sequence of visits to the 3D regions.

III. PROBLEM STATEMENT

The studied **3D Dubins Traveling Salesman Problem with Neighborhoods** (3D-DTSPN) stands to find a shortest trajectory which visits the given set of target regions that satisfies the motion constraints of the utilized *Dubins Airplane model* [6], i.e., the minimum turning radius and the limited pitch angle. A target region is considered to be successfully visited if the found trajectory has an intersection with the target region.

A. Dubins Airplane Model

A state q of the *Dubins Airplane model* is defined by its position $p = (x, y, z)$, $p \in \mathbb{R}^3$, heading angle θ, and pitch angle ψ, i.e., $q = (p, \theta, \psi)$. The configuration space $\mathcal{C} = \mathbb{R}^3 \times \mathbb{S}^2$ has five dimensions, and the motion of the vehicle is constrained by:

1) minimal turning radius ρ,
2) limited pitch angle, i.e., $\psi \in [\psi_{min}, \psi_{max}]$.

Hence, the **Dubins airplane model** is defined as:

$$\begin{bmatrix}\dot{x}\\ \dot{y}\\ \dot{z}\\ \dot{\theta}\end{bmatrix} = v\begin{bmatrix}\cos\theta\cdot\cos\psi\\ \sin\theta\cdot\cos\psi\\ \sin\psi\\ u_\theta\cdot\rho^{-1}\end{bmatrix}, \tag{1}$$

where v is a constant forward velocity of the aircraft and u_θ is the control input $u_\theta \in [-1, 1]$.

Although the model does not fully describe a real airplane dynamics, it seems to be a sufficient model for most fixed-wing airplanes that cannot perform acrobatic maneuvers [6].

B. Problem Definition of the 3D-DTSPN

Having a set of target regions $\mathcal{R} = (R_1, \ldots, R_n)$ in 3D, $R_i \subset \mathbb{R}^3$, the 3D-DTSPN stands to find a shortest closed-loop trajectory for the Dubins airplane which visits all the given regions. The trajectory is defined by a vector of visiting states $\mathcal{Q} = (q_1, \ldots, q_n)$ corresponding to the given regions and the permutation $\Sigma = (\sigma_1, \ldots, \sigma_n)$ of their visits, i.e., $1 \leq \sigma_i \leq n$. The method for generating 3D maneuvers is expected to be deterministic, and thus the 3D-DTSPN is defined as the optimization problem for the *Dubins Airplane model* (1):

$$\begin{aligned} &minimize_{\Sigma,\mathcal{Q}} && \sum_{i=1}^{n-1} \mathcal{L}(q_{\sigma_i}, q_{\sigma_{i+1}}) + \mathcal{L}(q_{\sigma_n}, q_{\sigma_1}) \\ &subject\ to && q_i = (p_i, \theta_i, \psi_i), \quad i = 1, \ldots, n, \\ & && p_i \in R_i, \qquad\qquad\quad i = 1, \ldots, n, \end{aligned} \tag{2}$$

where $\mathcal{L}(q_i, q_j)$ is the length of the 3D Dubins maneuver from q_i to q_j.

C. Dubins maneuver in 3D

The 3D trajectory generation procedure for the *Dubins Airplane model* (1) is adopted from [6] which extends the original work of [28] for fixed-wing UAVs. The trajectory is generated based on the 2D Dubins maneuver where the segments are then extended into 3D, see Fig. 2. If the altitude difference is too high, an additional spiral segment is inserted to gain the required altitude. Thus, the maneuvers are divided into *low/high/medium* altitude cases.

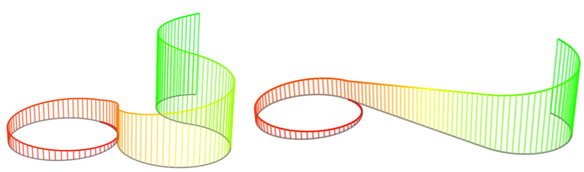

(a) CCC maneuver (b) CSC maneuver

Fig. 2. An example of 3D trajectories for the *Dubins Airplane model*.

For the *low altitude* case, the length of the generated 2D Dubins maneuver enables to gain the terminal altitude while the pitch angle constraint is met. Therefore, the original maneuver is directly extended into the 3D maneuver such that the altitude changes proportionally along the maneuver.

For the *high altitude* case, the 2D maneuver length is not sufficient to gain the required altitude. The original 2D maneuver is modified by inserting additional spiral segments at the start of the maneuver. The number of spiral segments depends on the required altitude change [6].

The *medium altitude* case combines both previous cases. The 2D length is not sufficient, but an additional spiral segment would be too long. In this case, a third turning segment is inserted to achieve the required prolongation. A detailed description of the procedure is provided in [6].

IV. Sampling-based Approach to the 3D-DTSPN

The sampling-based approach adopted from [4] addresses the continuous optimization part of the 3D-DTSPN by sampling the waypoint locations and heading angles. The configurations are selected from the four-dimensional space, i.e., a 3D position in the target region together with the corresponding heading angle. The pitch angle is not sampled, since it may change instantly in the *Dubins Airplane model*. Note that for each sample of the possible waypoint location, additional sampling of the possible heading angle at the waypoint is performed, and the number of samples is quickly increasing.

After the sampling, all trajectories connecting every possible pair of the sampled configurations are determined in $\mathcal{O}((nk)^2)$ steps for n target regions and k samples per region. Then, the problem is transformed to the strictly combinatorial Generalized Asymmetric TSP (GATSP) where the requested solution visits only a single sample per each region. Finally, the GATSP is transformed to the Asymmetric TSP (ATSP) using Noon-Bean transformation [35] and the ATSP can be solved by, e.g., [17], [18].

There are two main disadvantages of the sampling-based approach. First, the samples are selected from a high-dimensional configuration space, and many samples are necessary to find a solution of satisfiable quality, i.e., close to the optimal solution. Secondly, the problem is transformed to a relatively large instance of the Asymmetric TSP which is known to be NP-hard. Although heuristic approaches such as the LKH [18] exist, it is still computationally demanding, and only a limited number of samples can be used.

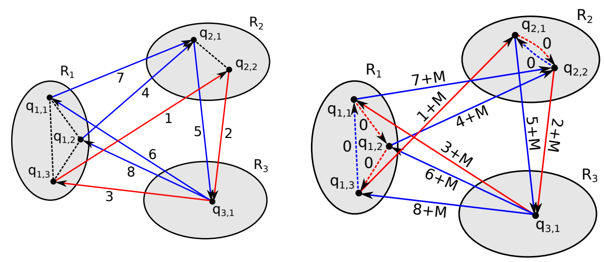

(a) GATSP instance (b) ATSP instance

Fig. 3. An example of the Noon-Bean transformation where edges from the optimal solution are in the red and the rest of the edges are in blue.

Once configurations are sampled and connecting trajectories are computed, the 3D-DTSPN is transformed into GATSP that is then transformed to the ATSP by the Noon-Bean transformation [35]. In the ATSP, all samples are visited but samples from the same set, i.e., corresponding to the same target regions, are connected by a zero-length cycle to preserve the solution of the GATSP. The edges between different sets are redirected such that the final trajectory remains feasible and a big constant M is added to the edge value to prevent re-entering to the same set twice. An example of the Noon-Bean transformation with three sets and six samples is depicted in Fig. 3. The example also illustrates how quickly the problem grows with each additional sample.

V. Proposed Solution of the 3D-DTSPN

The proposed solution of the introduced 3D-DTSPN is based on the decoupled approach adopted from [1] in which a sequence of visits to the target regions is determined before the trajectory generation. In contrast to the original work based on Euclidean distance, we propose a modified distance function that considers the constraints of the *Dubins Airplane model*. The sequence is used to generate an initial solution of the 3D-DTSPN which is further improved by an extended version of the Local Iterative Optimization (LIO) method adopted from [8]. The particular steps are described in the following paragraphs.

A. Finding a Sequence of Visits to the Target Regions

The sequence of visits to the target regions is determined concerning the distances between the centers of the target regions. The existing approaches for the DTSP such as [1], [13], [14], [15] utilize Euclidean distance to estimate the final trajectory cost, but they do not consider the minimum turning radius constraint. The problem is transformed to a solution of the TSP that can be solved by existing solvers.

The very same approach with the Euclidean distance can be used even for the 3D-DTSPN, but a sequence does not reflect the motion constraint on the pitch angle, especially if the target regions are close to each other while the altitude differences are high. In such cases, additional spiral segments are necessary to gain the terminal altitude, which prolongs the final path. Therefore, we propose to replace the Euclidean distance from the target locations c_i to c_j by the following distance function $d(c_i, c_j)$:

$$d(c_i, c_j) = \max\left(\|c_i - c_j\|, \frac{z_{c_j} - z_{c_i}}{\sin(\psi_{lim})}\right), \qquad (3)$$

where c_i stands for the center of the i-th target region, z_{c_i} for its height, and $\|.\|$ represents the Euclidean distance. The angle ψ_{lim} differs based on the altitude change, i.e., $\psi_{lim} = \psi_{min}$ for $z_{c_i} > z_{c_j}$ and $\psi_{lim} = \psi_{max}$ otherwise.

B. Finding a Solution and Local Optimization

Having the sequence of visits, the initial solution of the 3D-DTSPN is created by choosing a random vehicle configuration q_i described by its position p_i and heading angle θ_i for each target region R_i. The resulting trajectory has to intersect the boundary of each target region. Therefore only configurations on the boundary can be considered, which can encode an arbitrary solution while providing a significant simplification. The position is specified by two variables α and β, see Fig. 4.

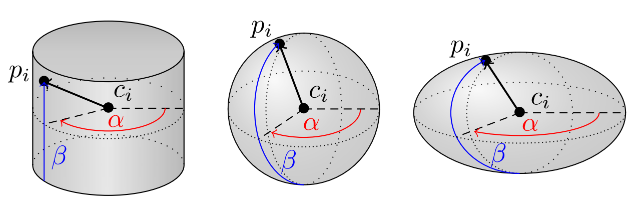

Fig. 4. The position p_i of the waypoint on the boundary of the target region is given by α and β which stands for the angle and relative height.

The 3D-DTSPN with the known sequence can be seen as a continuous optimization problem of $3n$ variables, i.e., the triplet (θ, α, β) for each visiting configuration. A solution to such a problem can be quickly computationally intractable with increasing number of the target regions n. Therefore, we propose to utilize the LIO method [8] which splits the problem into optimization sub-problems that are solved independently. This process is iteratively repeated until the solution stops improving. The full scheme of the proposed approach for the 3D-DTSPN is depicted in Algorithm 1.

Algorithm 1: Proposed algorithm for 3D-DTSPN

Data: Regions $\mathcal{R}$
Result: Solution represented by $\mathcal{Q}$ and Σ
$\Sigma \leftarrow$ getInitialSequence($\mathcal{R}$)
$\mathcal{Q} \leftarrow$ getInitialSolution($\mathcal{R}, \Sigma$)
while *terminal condition* **do**
    $\mathcal{Q} \leftarrow$ optimizeHeadings($\mathcal{Q}, \mathcal{R}, \Sigma$)
    $\mathcal{Q} \leftarrow$ optimizeAlpha($\mathcal{Q}, \mathcal{R}, \Sigma$)
    $\mathcal{Q} \leftarrow$ optimizeBeta($\mathcal{Q}, \mathcal{R}, \Sigma$)
end
return $\mathcal{Q}, \Sigma$

First, the algorithm determines the sequence Σ and generates the initial solution with random waypoints on the target region boundaries; the LIO-based solver iteratively improves the trajectory. The LIO procedure is divided into three separate steps based on the optimized variable. Furthermore, all these steps are repeated until the solution converges, i.e., the improvement is not significant. Thus, in each iteration of the local optimization, all three variables $(\theta_i, \alpha_i, \beta_i)$ determining the waypoint q_i are updated. Finally, after a given number of steps or when the solution is not improving, the algorithm returns the final solution. Notice, the first solution is found very quickly, and it is then improved in further iterations, and thus the proposed algorithm has the any-time property and can be eventually employed in real-time planning.

VI. Results

The proposed approaches for the 3D-DTSPN have been evaluated on randomly generated 3D scenarios with cylindrical target regions. The minimum turning radius $\rho = 1$ and centers of the regions are uniformly distributed in the given cubical bounding box and both the region radius and height are randomly chosen from the interval [0, 2]. The vertical size of the bounding box is fixed to 10, and its horizontal size b_h depends on the number of targets together with the average region density ω by the following equation:

$$b_h = \sqrt{\frac{n}{\omega}}. \qquad (4)$$

The pitch angle of the vehicle is limited to be in the interval $\psi \in [-15°, 20°]$ to reflect the behavior of the real fixed-wing vehicles which typically have an asymmetric interval for the pitch angle. An example of the evaluated 3D-DTSPN instance with 20 cylindrical target regions is depicted in Fig. 5. Notice the found target sequence differs from the one that would be found as a solution of the Euclidean TSP.

The proposed decoupled algorithm is denoted `Proposed+LIO` in which the distance function is

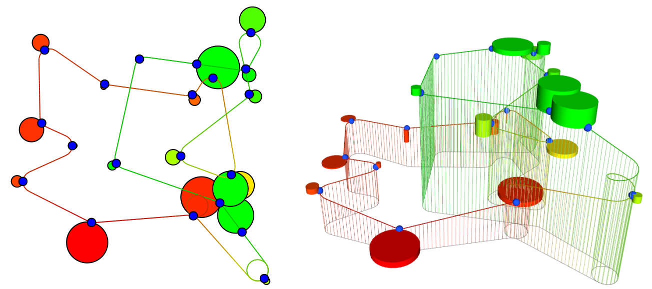

(a) 2D projection (b) 3D projection

Fig. 5. An example instance of the 3D-DTSPN with $n = 20$ target regions and target density $\omega = 0.03$.

specially designed for the *Dubins Airplane model* (1), and the generated TSP is solved by the heuristic LKH solver [18]. The final trajectory is optimized by LIO with the maximum of 10 iterations of the main loop in Algorithm 1.

The proposed decoupled algorithm is compared with two other approaches. First, we consider finding the sequence of visits as a solution of the Euclidean TSP to show benefits of the proposed distance function (3) to the solution quality. This approach is denoted `ETSP+LIO`. Besides, we also consider the sampling-based approach described in Section IV for which we use the same LKH solver as for the sequencing part of the decoupled approaches. The approach is denoted `Sampling` with the suffix specifying the number of samples on the boundary of each target region to show the effect of the increasing number of samples to the solution quality and also the required computational time. All the algorithms have been implemented in C++ and executed on a single core of the Intel Core i5-7600K CPU running at 3.80 GHz.

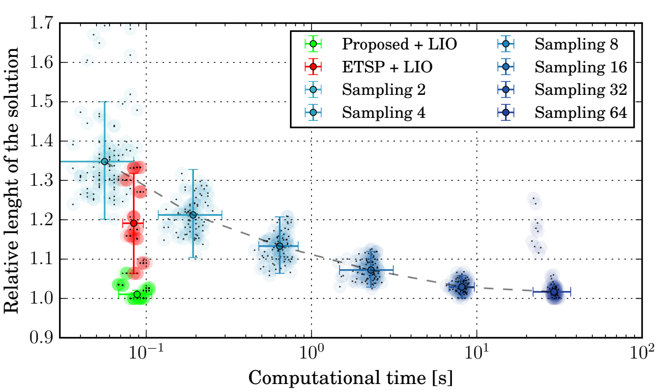

Fig. 6. The relative length of the solution over time for 20 target regions with the density $\omega = 0.03$. The median and 90% non-parametric confidence interval are computed from 10 random instances each with 10 trials.

In the first scenario, all three approaches are compared in the solution of the 3D-DTSPN instances with $n = 20$ target regions. The average performance indicators from 10 trials on 10 randomly generated instances are depicted in Fig. 6. The trajectory lengths are normalized separately for each problem instance using the best-found solution from all the trials and approaches, which allows to aggregate the results and present them in a single plot. The results indicate that the proposed decoupled method provides about 20%

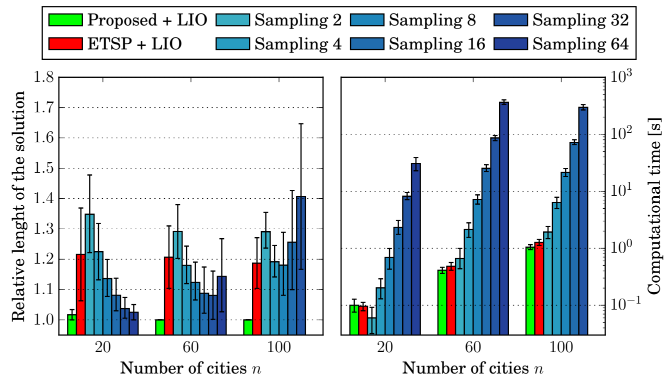

Fig. 7. Relative solution length and computational time for problems with the number of regions n and target density $\omega = 0.03$. (Median and 90% non-parametric confidence interval from 5 random instances with 10 trials.)

shorter solutions than both other approaches for the same computational time. It is also about two orders of magnitude faster than the sampling-based approach in finding solutions with the similar quality. It can be noticed that for few cases the ETSP+LIO may also provide good solutions; however, in most cases, the proposed heuristic distance function (3) provides significantly better results.

The approaches have been further evaluated on larger problems with $n \in \{20, 60, 100\}$ and the target regions density $\omega = 0.03$. The average quality indicators are presented in Fig. 7. The results show that the proposed approach can find solutions with reasonable quality (regarding the solutions found for a high number of samples) even for a high number of target regions, e.g., in about 1 seconds for 100 regions.

The sampling-based algorithm quickly becomes computationally demanding for the increasing number of regions or samples. Notice the logarithmic axis of the computational time. It is a bit surprising that the relative solution length increased for the sampling-based approach. Based on the analysis, this behavior is caused by the Noon-Bean transformation in which a relatively big constant is added to the final length, which causes a numeric instability of the ATSP solver. Such a problem is especially noticeable for 64

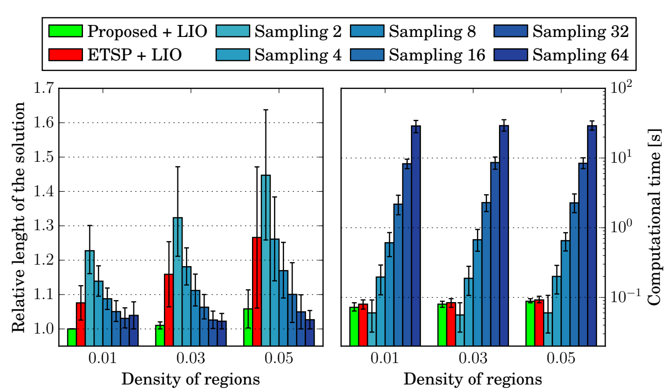

Fig. 8. Relative length of the solutions and average required computational times for 3D-DTSPN instances with the target regions density ω and $n = 20$ targets. (Median and 90% non-parametric confidence interval from 5 random instances with 10 trials.)

samples in Fig. 6, where the constant M is very high because of many nodes in the graph representation of the problem.

Finally, the approaches for the 3D-DTSPN have been evaluated on instances with various targets densities. The results are depicted in Fig. 8. According to the presented results, the proposed decoupled approach with the distance function (3) provides the superior results, especially in problems with a high density of the target regions. In contrast, the decoupled approach with the Euclidean distance provides solutions with similar quality only for the low densities of the regions. The sampling-based algorithm struggles in problem instances with high densities of the regions when the number of samples is low, but this can be addressed by using more samples at the cost of the significantly increased computational requirements.

VII. Conclusion

An extension of the Dubins TSPN into the three-dimensional space using the *Dubins Airplane model* is proposed in this paper. The problem can be addressed by a modification of existing sampling-based approach for the DTSPN; however, the configuration space is of the dimension five, and this approach suffers from its high computational requirements even for small 3D instances. Therefore, the decoupled approach is considered with the newly proposed distance cost function to reflect different altitudes of the target regions and the motion constraints of the utilized *Dubins Airplane model*. Based on empirical evaluations, the proposed approach provides solutions with about 20% shorter paths in comparison to the sampling-based approach for the same computational time. Besides, it is about two orders of magnitude faster than the sampling-based approach in finding solutions with the competitive solution quality.

References

[1] K. Savla, E. Frazzoli, and F. Bullo, "On the point-to-point and traveling salesperson problems for dubins' vehicle," in *Proceedings of the American Control Conference*. IEEE, 2005, pp. 786–791.

[2] J. Faigl, P. Váňa, M. Saska, T. Báča, and V. Spurný, "On solution of the dubins touring problem," in *ECMR*, 2017, pp. 1–6.

[3] J. T. Isaacs, D. J. Klein, and J. P. Hespanha, "Algorithms for the traveling salesman problem with neighborhoods involving a dubins vehicle," in *American Control Conference*, 2011, pp. 1704–1709.

[4] K. Obermeyer, P. Oberlin, and S. Darbha, "Sampling-based roadmap methods for a visual reconnaissance uav," in *AIAA Guidance, Navigation, and Control Conference*, 2010, p. 7568.

[5] D. G. Macharet, A. A. Neto, V. F. da Camara Neto, and M. F. Campos, "Data gathering tour optimization for dubins' vehicles," in *IEEE Congress on Evolutionary Computation (CEC)*, 2012, pp. 1–8.

[6] M. Owen, R. W. Beard, and T. W. McLain, "Implementing dubins airplane paths on fixed-wing uavs," in *Handbook of Unmanned Aerial Vehicles*. Springer, 2015, pp. 1677–1701.

[7] P. Oberlin, S. Rathinam, and S. Darbha, "Today's traveling salesman problem," *Robotics & Automation Magazine, IEEE*, vol. 17, no. 4, pp. 70–77, 2010.

[8] P. Váňa and J. Faigl, "On the dubins traveling salesman problem with neighborhoods," in *IROS*. IEEE, 2015, pp. 4029–4034.

[9] L. E. Dubins, "On curves of minimal length with a constraint on average curvature, and with prescribed initial and terminal positions and tangents," *American Journal of mathematics*, vol. 79, no. 3, pp. 497–516, 1957.

[10] X. Bui, J. Boissonnat, J. Laumond, and P. Soures, "The shortest path synthesis for non-holonomic robots moving forwards, inria, nice-sophia-antipolis," Research Report 2153, Tech. Rep., 1994.

[11] X. Goaoc, H.-S. Kim, and S. Lazard, "Bounded-curvature shortest paths through a sequence of points using convex optimization," *SIAM Journal on Computing*, vol. 42, no. 2, pp. 662–684, 2013.

[12] A. Dumitrescu and J. S. B. Mitchell, "Approximation algorithms for tsp with neighborhoods in the plane," in *Proceedings of the Twelfth Annual ACM-SIAM Symposium on Discrete Algorithms*. Society for Industrial and Applied Mathematics, 2001, pp. 38–46.

[13] X. Ma and D. A. Castanon, "Receding horizon planning for dubins traveling salesman problems," in *Proceedings of the 45th IEEE Conference on Decision and Control*. IEEE, 2006, pp. 5453–5458.

[14] K. Savla, E. Frazzoli, and F. Bullo, "Traveling salesperson problems for the dubins vehicle," *IEEE Transactions on Automatic Control*, vol. 53, no. 6, pp. 1378–1391, 2008.

[15] D. G. Macharet, A. A. Neto, V. F. da Camara Neto, and M. F. Campos, "Nonholonomic path planning optimization for dubins' vehicles," in *ICRA*, 2011, pp. 4208–4213.

[16] R. Pěnička, M. Saska, C. Reymann, and S. Lacroix, "Reactive dubins traveling salesman problem for replanning of information gathering by uavs," in *ECMR*, 2017, pp. 1–6.

[17] D. Applegate, R. Bixby, V. Chvátal, and W. Cook, "CONCORDE TSP Solver," 2003, [cited 13 Sep 2017]. [Online]. Available: http://www.tsp.gatech.edu/concorde.html

[18] K. Helsgaun, "LKH solver 2.0.7," [cited 13 Sep 2017]. [Online]. Available: http://www.akira.ruc.dk/~keld/research/LKH/

[19] D. G. Macharet, A. A. Neto, V. F. da Camara Neto, and M. F. Campos, "An evolutionary approach for the dubins' traveling salesman problem with neighborhoods," in *14th annual conference on Genetic and evolutionary computation*. ACM, 2012, pp. 377–384.

[20] X. Zhang, J. Chen, B. Xin, and Z. Peng, "A memetic algorithm for path planning of curvature-constrained uavs performing surveillance of multiple ground targets," *Chinese Journal of Aeronautics*, vol. 27, no. 3, pp. 622–633, 2014.

[21] J. Faigl and P. Váňa, "Self-organizing map for the curvature-constrained traveling salesman problem," in *ICANN*, 2016, pp. 497–505.

[22] J. Faigl and P. Váňa, "Unsupervised learning for surveillance planning with team of aerial vehicles," in *IJCNN*, 2017, pp. 4340–4347.

[23] R. Pěnička, J. Faigl, P. Váňa, and M. Saska, "Dubins Orienteering Problem," *Robotics and Automation Letters*, vol. 2, no. 2, pp. 1210–1217, 2017.

[24] J. Faigl, "Self-organizing map for orienteering problem with dubins vehicle," in *WSOM+*, 2017, pp. 125–132.

[25] R. Pěnička, J. Faigl, P. Váňa, and M. Saska, "Dubins orienteering problem with neighborhoods," in *ICUAS*. IEEE, 2017, pp. 1555–1562.

[26] J. Faigl and R. Pěnička, "On close enough orienteering problem with dubins vehicle," in *IROS*, 2017, pp. 5646–5652.

[27] P. Váňa, J. Faigl, J. Sláma, and R. Pěnička, "Data collection planning with dubins airplane model and limited travel budget," in *ECMR*. IEEE, 2017, pp. 1–6.

[28] H. Chitsaz and S. M. LaValle, "Time-optimal paths for a dubins airplane," in *46th IEEE Conference on Decision and Control*. IEEE, 2007, pp. 2379–2384.

[29] H. J. Sussmann, "Shortest 3-dimensional paths with a prescribed curvature bound," in *Proceedings of the 34th IEEE Conference on Decision and Control*, vol. 4. IEEE, 1995, pp. 3306–3312.

[30] G. Ambrosino, M. Ariola, U. Ciniglio, F. Corraro, A. Pironti, and M. Virgilio, "Algorithms for 3d uav path generation and tracking," in *Proceedings of the 45th IEEE Conference on Decision and Control*. IEEE, 2006, pp. 5275–5280.

[31] S. Hota and D. Ghose, "Optimal path planning for an aerial vehicle in 3d space," in *Proceedings of the 49th IEEE Conference on Decision and Control*. IEEE, 2010, pp. 4902–4907.

[32] Y. Wang, S. Wang, M. Tan, C. Zhou, and Q. Wei, "Real-time dynamic dubins-helix method for 3-d trajectory smoothing," *IEEE Transactions on Control Systems Technology*, vol. 23, no. 2, pp. 730–736, 2015.

[33] A. A. Neto, D. G. Macharet, and M. F. M. Campos, "3d path planning with continuous bounded curvature and pitch angle profiles using 7th order curves," in *IROS*. IEEE, 2015, pp. 4923–4928.

[34] J. Faigl and P. Váňa, "Surveillance Planning with Bézier Curves," *IEEE Robotics and Automation Letters*, vol. 3, no. 2, pp. 750–757, April 2018.

[35] C. E. Noon and J. C. Bean, "A lagrangian based approach for the asymmetric generalized traveling salesman problem," *Operations Research*, vol. 39, no. 4, pp. 623–632, 1991.